ACCOUNTS of chemical research

pubs.acs.org/accounts Article

Physical Transformations of Noble-Metal Nanocrystals upon Thermal Activation

Published as part of the Accounts of Chemical Research special issue "Transformative Inorganic Nanocrystals".

Zhiheng Lyu,[⊥] Ruhui Chen,[⊥] Manos Mavrikakis, and Younan Xia*

Cite This: *Acc. Chem. Res.* 2021, 54, 1−10 Read Online

ACCESS | Metrics & More | Article Recommendations

CONSPECTUS: The last two decades have witnessed the successful development of noble-metal nanocrystals with well-controlled properties for a variety of applications in catalysis, plasmonics, electronics, and biomedicine. Most of these nanocrystals are kinetically controlled products greatly deviated from the equilibrium state defined by thermodynamics. When subjected to elevated temperatures, their arrangements of atoms are expected to undergo various physical transformations, inducing changes to the shape, morphology (hollow vs solid), spatial distribution of elements (segregated vs alloyed/intermetallic), internal structure (twinned vs single-crystal), and crystal phase. In order to optimize the performance of these nanocrystals in various applications, there is a pressing need to understand and improve their thermal stability.

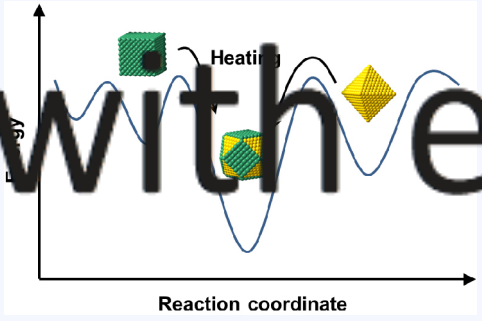

By integrating in situ heating with transmission electron microscopy or X-ray diffraction, we have investigated the physical transformations of various types of noble-metal nanocrystals in real time. We have also explored the atomistic detail responsible for a physical transformation using first-principles calculations, providing insightful guidance for the development of noble-metal nanocrystals with augmented thermal stability. Specifically, solid nanocrystals were observed to transform into pseudospherical particles favored by thermodynamics by reducing the surface area while eliminating the facets high in surface energy. For nanocrystals of relatively large in size, a single-crystal lattice was more favorable than a twinned structure. When switching to core−shell nanocrystals, the elevation in temperature caused changes to the elemental distribution in addition to shape transformation. The compositional stability of a core−shell nanocrystal was found to be strongly dependent on the shape and thus the type of facet expressed on the surface. For hollow nanocrystals such as nanocages and nanoframes, their thermal stabilities were typically inferior to the solid counterparts, albeit their unique structure and large specific surface area are highly desired in applications such as catalysis. When a metastable crystal structure was involved, phase transition was also observed at a temperature close to that responsible for shape or compositional change. We hope the principles, methodologies, and mechanistic insights presented in this Account will help the readers achieve a good understanding of the physical transformations that are expected to take place in noble-metal nanocrystals when they are subjected to thermal activation. Such an understanding may eventually lead to the development of effective methods for retarding or even preventing some of the transformations.

KEY REFERENCES

- Gilroy, K. D.; Elnabawy, A. O.; Yang, T. H.; Roling, L. T.; Howe, J.; Mavrikakis, M.; Xia, Y. Thermal Stability of Metal Nanocrystals: An Investigation of the Surface and Bulk Reconstructions of Pd Concave Icosahedra. *Nano Lett.* **2017**, *17*, 3655−3661.[1] *This work analyzed the thermal stability of nanocrystals in terms of morphology and internal structure (twinned vs single-crystal). The Pd concave icosahedron evolved into a regular icosahedron via surface reconstruction upon heating to 200−400 °C and then transformed into a pseudospherical, single-crystal particle through bulk reconstruction when further heated to 600 °C.*
- Vara, M.; Roling, L. T.; Wang, X.; Elnabawy, A. O.; Hood, Z. D.; Chi, M.; Mavrikakis, M.; Xia, Y. Understanding the Thermal Stability of Palladium-Platinum Core-Shell Nanocrystals by *In Situ* Transmission Electron Microscopy and Density Functional Theory. *ACS Nano* **2017**, *11*, 4571−4581.[2] *This work investigated the thermal stability of Pd@Pt_{4L} core−shell nanocrystals in terms of shape and composition (segregated vs alloyed). A dependence on the initial shape (or facet) of*

Received: October 1, 2020
Published: December 4, 2020

https://dx.doi.org/10.1021/acs.accounts.0c00640
Acc. Chem. Res. 2021, 54, 1−10

the nanocrystals was observed, with the deformation of the cube occurring at a temperature 400 °C lower than the octahedral shape, whereas the alloying between the Pd core and Pt shell of an octahedron occurred at a temperature 200 °C lower than that for the cubic counterpart.

- Zhao, M.; Chen, Z.; Lyu, Z.; Hood, Z. D.; Xie, M.; Vara, M.; Chi, M.; Xia, Y. Ru Octahedral Nanocrystals with a Face-Centered Cubic Structure, {111} Facets, Thermal Stability up to 400 °C, and Enhanced Catalytic Activity. *J. Am. Chem. Soc.* **2019**, *141*, 7028−7036.[3] *This work examined the thermal stability of Rh@Ru core−shell octahedra in terms of shape and crystal structure. At a temperature around 500 °C, the octahedron started to show truncated corners while the crystal structure transformed from face-centered cubic (fcc) to hexagonal-close packed (hcp).*
- Zhao, M.; Xu, L.; Vara, M.; Elnabawy, A. O.; Gilroy, K. D.; Hood, Z. D.; Zhou, S.; Figueroa-Cosme, L.; Chi, M.; Mavrikakis, M.; Xia, Y. Synthesis of Ru Icosahedral Nanocages with a Face-Centered-Cubic Structure and Evaluation of Their Catalytic Properties. *ACS Catal.* **2018**, *8*, 6948−6960.[4] *This work evaluated the thermal stability of Ru icosahedral nanocages in terms of crystal structure (fcc vs hcp) and morphology (hollow vs solid). At a temperature around 350 °C, the crystal structure transformed from fcc to hcp due to the ultrathin walls, in addition to the fragmentation of the nanocage into multiple solid pieces.*

1. INTRODUCTION

Thermodynamics and kinetics both play important roles in determining the arrangement of atoms in a solid material. While thermodynamics defines the most stable arrangement with the lowest total free energy, kinetics controls the path and time scale in reaching the thermodynamic state. During the synthesis of a solid material, the arrangement of atoms can be arrested at local minima, generating metastable or kinetically controlled products (Figure 1A).[5] Remarkably, the kinetically controlled products can persist over long periods and even find use in applications. A classic example can be found in diamond, a metastable allotrope of carbon that is supposed to spontaneously transform into graphite under ambient conditions (Figure 1B). In reality, however, the transformation kinetics is so slow that diamond can last "forever" once it has been synthesized. As a matter of fact, diamond has found use in a variety of industrial applications, even though it is a metastable, far-from equilibrium material.[6,7] While the direction of a transformation is set by thermodynamics, it is kinetics that controls the rate and thereby the duration of time necessary for completing the transformation. The kinetics is, in turn, controlled by temperature. According to Arrhenius equation ($k = A\, e^{-E_a/RT}$), the rate constant k is determined by the ratio between the activation energy (E_a) and the thermal energy (temperature, T).[5] When a kinetically controlled product is subjected to thermal activation, its transformation into the equilibrium state will be greatly accelerated. In addition to direct heating, the temperature can also be elevated through the application of light irradiation or ultrasonication.[8−10]

In the case of noble-metal nanocrystals, the transformation of atomic arrangement can arise from variations in shape, morphology, composition, and/or internal structure, as well as

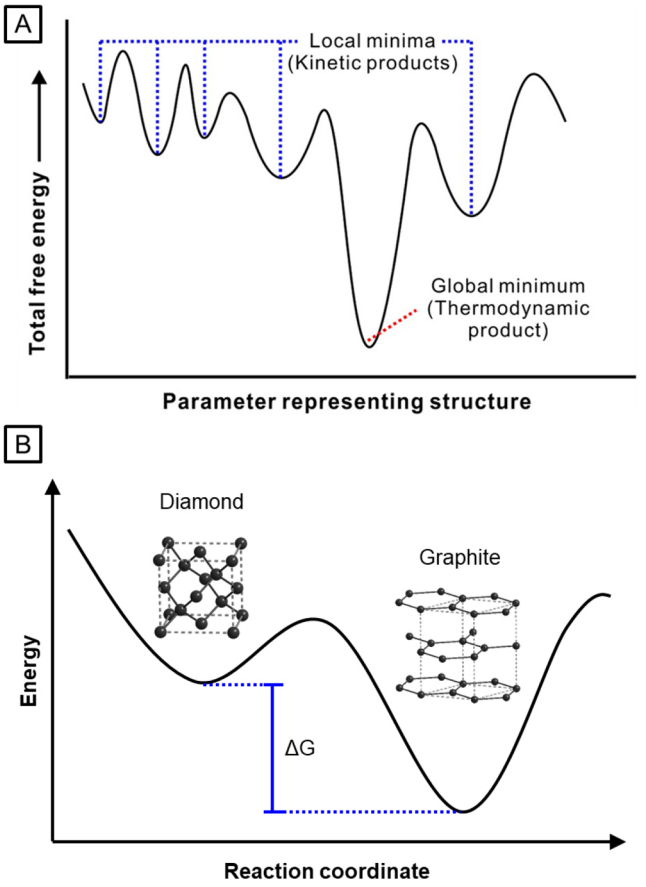

Figure 1. (A) Schematic illustration showing the formation of kinetically controlled products being trapped at various local minima relative to the thermodynamic product located at the global minimum in terms of total free energy. (B) Schematic illustration showing graphite as a thermodynamically more favorable material than diamond under ambient conditions. ΔG represents the change in Gibbs free energy for the transformation from diamond to graphite. (A) Reproduced with permission from ref 5. Copyright 2015 American Chemical Society.

the crystal phase. Figure 2 shows three examples of physical transformations that noble-metal nanocrystals typically experience when they are subjected to elevated temperatures, including shape deformation, change in elemental distribution, and fragmentation. Other transformations such as changes to the internal structure and/or crystal phase may also occur. In some cases, all these five types of transformations can take place in the same particle, at similar or different temperatures. It should be pointed out that many catalytic reactions involving noble-metal nanocrystals are conducted at elevated temperatures, with notable examples including the Fischer−Tropsch process (150−300 °C),[11] CO oxidation (25−300 °C),[12] water gas shift reaction (200−450 °C),[13] and ammonia synthesis (400−600 °C).[14] As such, it is of critical importance to understand how the noble-metal nanocrystals will behave upon heating by uncovering the mechanistic details underlying various types of physical transformations. Such an understanding will aid the rational development of strategies for enhancing the thermal stability of noble-metal nanocrystals.

Here we offer an account of recent progress in understanding the transformations of noble-metal nanocrystals when they are subjected to thermal activation. We begin with a discussion on the changes to shape and internal structure of

https://dx.doi.org/10.1021/acs.accounts.0c00640
Acc. Chem. Res. 2021, 54, 1−10

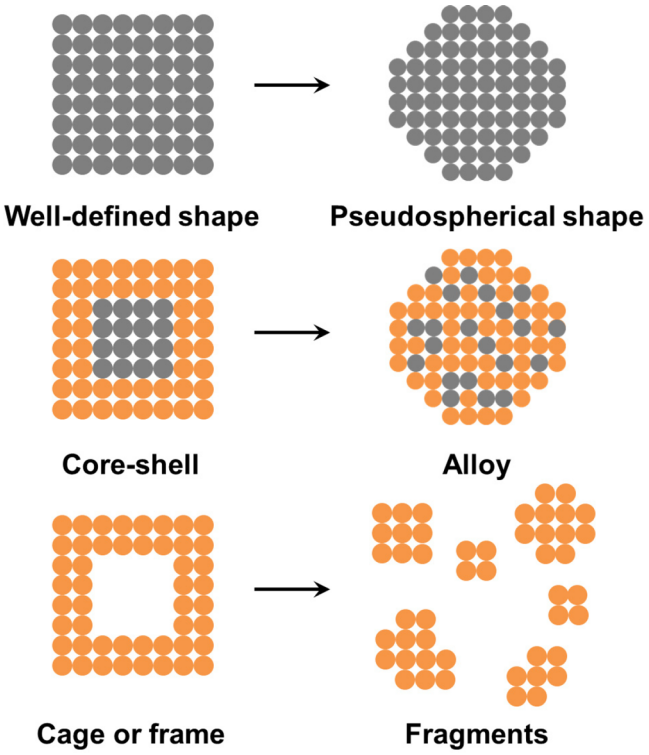

Figure 2. Schematic illustration showing different types of physical transformations in terms of shape, elemental distribution, or morphology when noble-metal nanocrystals are subjected to thermal activation.

solid monometallic nanocrystals, and then extend the scope to core−shell and hollow nanocrystals. For the latter two systems, the transformations are dominated by variation in elemental distribution and fragmentation, respectively. Depending on the metals involved, phase transition may also occur. Throughout our discussion, we pay close attention to the mechanistic detail of each transformation, as well as the possible strategies for retarding or preventing the transformation.

2. SOLID MONOMETALLIC NANOCRYSTALS

For solid monometallic nanocrystals, the most commonly observed transformation is the changes to shape or morphology as a result of truncation at corners and edges. Such a transformation will be sped up when the nanocrystals are subjected to elevated temperatures because of the acceleration in atom diffusion. In an early study, we investigated the shape transformation of Pd nanocubes when heated to 500 °C for 1 h in a high-resolution transmission electron microscope (TEM).[15] Significant truncation occurred to the corners, as revealed by the enlargement of {111} facets and shrinkage of {100} facets. Such an observation implied the migration of atoms from corners to side faces (Figure 3A). For a face-centered cubic (fcc) metal, the surface free energies of the low-index facets decrease in the order of $\gamma_{\{110\}} > \gamma_{\{100\}} > \gamma_{\{111\}}$ in the absence of capping agent.[5] As a result, truncating the corners and thus enlarging the {111} facets are favored by thermodynamics as it will reduce the total surface free energy of the particle. In addition to corner truncation, surface reconstruction was also observed during thermal annealing. Owing to the involvement of atomic addition in the growth of nanocubes, several types of surface defects, including adatom islands, vacancy pits, and steps, tended to form on the side

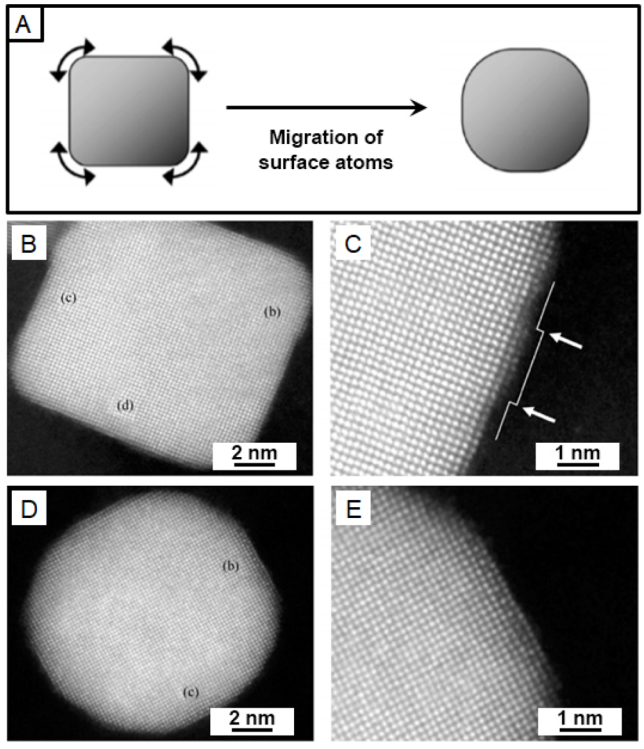

Figure 3. (A) Schematic illustration showing the migration of surface atoms on a Pd nanocube during the annealing process. (B) High-angle annular dark-field scanning transmission electron microscopy (HAADF-STEM) image of an as-prepared, single Pd nanocube. (C) Magnified image of the selected region (b) in panel (B). (D) HAADF-STEM image of a Pd nanocube after annealing at 500 °C for 1 h. (E) Magnified image of the selected region (b) in panel (D). An acceleration voltage of 200 kV was used for STEM imaging. Reproduced with permission from ref 15. Copyright 2010 Springer Nature.

faces (Figure 3B and C). These defects disappeared during thermal annealing for the creation of a smooth surface, suggesting the involvement of surface reconstruction (Figure 3D and E). Because of their lower coordination numbers and thus higher energies relative to those atoms situated on a perfect surface, the defects are not favored by thermodynamics, providing a major driving force for their removal during the annealing process.

Along with the shape transformation, thermal annealing can also induce changes to the internal structure of nanocrystals for the elimination of twin defects.[1] To this end, we examined the thermal stability of twinned nanocrystals with a concave shape, which have attracted extensive attention in catalysis due to the presence of a large proportion of low-coordination atoms, high-index facets, and lattice strain.[16] Such nanocrystals are far from equilibrium in terms of either surface or volume energy and are susceptible to physical transformations when subjected to elevated temperatures. We investigated the thermal stability of Pd concave icosahedra (Figure 4A) in real time through the use of high-resolution TEM equipped with in situ heating capability.[1] At room temperature, the angle between adjacent facets was found to vary between 120° and 160°, confirming a concave surface (Figure 4B). As the temperature was increased to 200 °C, concavity decreased as revealed by the increase in angle between adjacent facets. The trend became more obvious when the temperature reached 400 °C, at which point the

https://dx.doi.org/10.1021/acs.accounts.0c00640
Acc. Chem. Res. 2021, 54, 1−10

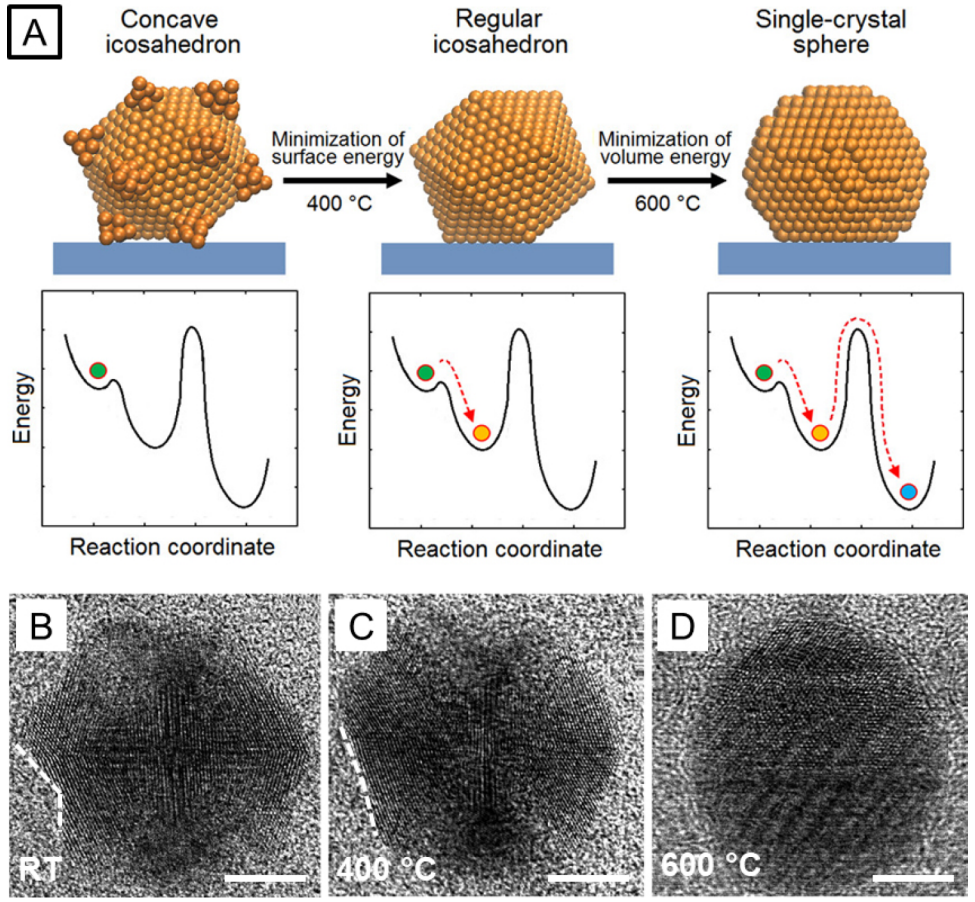

Figure 4. (A) Schematic illustration showing the transformations of shape and internal structure for a Pd concave icosahedron when heated to different temperatures, together with the energy diagram of the nanocrystal at each stage. (B–D) High-resolution TEM images (acceleration voltage: 200 kV) showing the transformation of an individual Pd nanocrystal from (B) a concave icosahedron (23 °C) to (C) a regular icosahedron (400 °C), and finally (D) a single-crystal structure (600 °C). The scale bars are 5 nm. Reproduced with permission from ref 1. Copyright 2017 American Chemical Society.

overall shape of the nanocrystal became a regular icosahedron but with a rounded profile due to the truncation at corners (Figure 4C). Upon heating, the Pd atoms situated at the tips of a concave icosahedron quickly gained adequate kinetic energy to migrate across the surface and settled onto side faces, so the total surface free energy of the particle would be reduced. Up to 400 °C, the twin defects remained largely intact because of the greater barrier to atom diffusion in the bulk than on the surface.

Elevating the temperature further to 600 °C led to more dramatic changes. When the atoms in the bulk gained enough kinetic energy to eliminate the twin defects and alleviate the strain energy, the icosahedron evolved into a single-crystal particle favored by thermodynamics (Figure 4D).[1] As such, both the total surface free energy and volume energy are minimized. Based on theoretical calculations, Pd icosahedra are only stable at a size smaller than 1.5 nm, corresponding to around 100 atoms or fewer.[17,18] In comparison, decahedral and single-crystal particles are thermodynamically more favorable for nanocrystals with sizes of 1.5–6 and >6 nm (i.e., 100–6500 and more than 6500 atoms), respectively. For icosahedra and decahedra, the excess energy caused by strain increases as the nanocrystals get larger, contributing to their intrinsic thermal instability. Similar structural reorganization was also reported for FePt icosahedra under electron beam flux.[19] Upon irradiation by a high dose of electrons (~200 A/cm^2 at an acceleration voltage of 300 kV), corner truncation occurred, followed by their melting and recrystallization into a single-crystal structure.

To quantitatively analyze the diffusion of atoms across the surface of a Pd concave icosahedron, density functional theory (DFT) calculations were conducted and the surface concavity was represented by a series of steps.[1] It was found that the activation energy barriers for the key steps in the transformation, such as the ejection of atoms out of steps and their diffusion downward to a subsequent step, could be overcome at 200 °C, in agreement with the experimental observation. Given the thermodynamics of all possible stepwise removal sequences, the topmost layer would be removed first, starting from the most undercoordinated atoms located at edges, followed by the removal of the underlying, incomplete layers. Interestingly, as the number of the eliminated atomic rows increased, the activation energy for ejecting a step edge atom decreased as well. In other words, once the deformation started, a decreasing resistance would be experienced in transforming to a less concave structure, explaining the swift reconstruction of the concave icosahedron.

3. SOLID CORE–SHELL NANOCRYSTALS

Core–shell nanocrystals have received ever increasing interest for applications in catalysis and plasmonics.[20–22] Despite the significant progress in controlling the synthesis of core–shell

https://dx.doi.org/10.1021/acs.accounts.0c00640
Acc. Chem. Res. 2021, 54, 1–10

nanocrystals with different combinations of elements, their compositional stability at elevated temperatures remains a major concern because of possible mixing between the atoms in the core and shell. In the presence of shape transformation, these two processes may even couple with each other, creating thermal behaviors different from those of monometallic nanocrystals.

By integrating high-resolution TEM with DFT calculations, we systematically investigated the shape-dependent thermal stability of Pd@Pt_{4L} core−shell nanocrystals.[2] The nanocubes were found to exhibit a reverse trend in terms of shape and compositional stability relative to their octahedral counterparts. Upon heating, the nanocubes started to lose their shape and smooth surface at 500 °C, while the octahedral sample could maintain its shape up until 900 °C (Figure 5A and B).

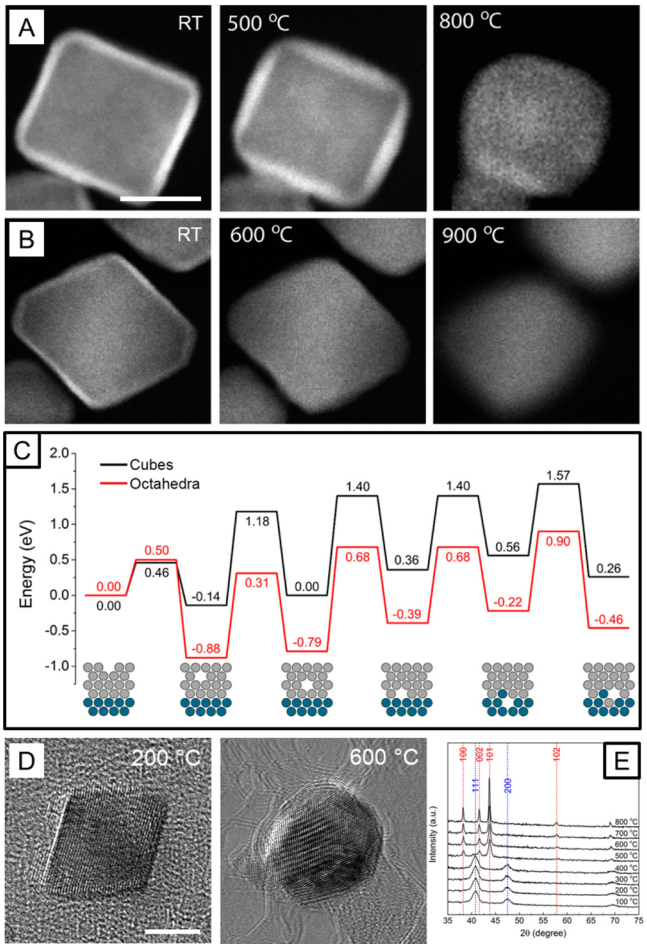

Figure 5. (A, B) HAADF-STEM images recorded from the same (A) Pd@Pt_{4L} cube and (B) Pd@Pt_{4L} octahedron under different heating conditions (acceleration voltage: 300 kV). The scale bar in (A) is 10 nm and applies to all other images in (A) and (B). (C) Energetics of subsurface vacancies in surface models of the Pd@Pt_{4L} nanocrystals. (D) High-resolution TEM images recorded from the same Rh@Ru octahedron under different heating conditions (acceleration voltage: 300 kV, electron dose rate: ∼ 10^6 e/nm^2·s). The scale bar is 5 nm and applies to both images in (D). (E) XRD patterns of fcc Rh@Ru octahedra heated to different temperatures. The characteristic peaks of fcc- and hcp-Ru are marked by blue and red dashed lines, respectively. Reproduced with permission from (A−C) ref 2 and (D, E) ref 3. Copyrights 2017 and 2019 American Chemical Society, respectively.

On the other hand, the nanocubes showed superior compositional stability, with the core−shell structure being preserved until 800 °C, 200 °C higher than the transition point for their octahedral counterparts. Our DFT calculations suggested that the shape stability of the core−shell nanocrystals was highly dependent on the facets expressed on the surface.[2] When moving an atom from the edge to an adjacent facet, the process was exothermic in the cubic model (ΔE = −0.15 eV) whereas highly endothermic for the octahedral model (ΔE = 1.64 eV), and the energy barrier (0.60 vs 1.99 eV) was much lower for (100) than that for (111). The difference in energetics can be ascribed to the lower coordination number for the edge atoms in a cube relative to that in an octahedron (5 vs 7). With fewer bonds connecting to neighboring atoms, the edge atoms in a cube have higher mobility, leading to shape deformation at a lower temperature. Moreover, the greater surface energy of (100) relative to (111) provides an additional driving force for the shape transformation of a nanocube.

Other than shape stability, DFT calculations revealed that the compositional stability of the core−shell nanocrystals was also dependent on the type of facet exposed on the surface.[2] It was suggested that the intermixing between the Pd atoms in the core and the Pt atoms in the shell was mediated by the subsurface vacancies incorporated into the nanocrystals during seed-mediated growth, which could reduce the energy barrier to atom diffusion (Figure 5C). Although the energy barriers for the subsurface vacancy formation were similar (0.46 vs 0.50 eV) for (100) and (111) facets, the process was more exothermic on (111) relative to (100) ($\Delta E_{(100)}$ = −0.14 eV vs $\Delta E_{(111)}$ = −0.88 eV). As such, a higher concentration of subsurface vacancies would be thermodynamically favored in octahedral nanocrystals, facilitating the interdiffusion of atoms and thus the loss of core−shell structure at a lower temperature relative to the cubic system. Additionally, ex situ heating experiments confirmed that both the Pd@Pt_{4L} cubes and octahedra could preserve their shapes and core−shell structures at a temperature up to 400 °C, demonstrating their great promise in thermal catalysis.

In addition to the transformations in shape and composition, the crystal structure of core−shell nanocrystals may undergo phase transition upon heating. To this end, we analyzed the thermal stability of Rh@Ru core−shell octahedral nanocrystals by TEM and X-ray diffraction (XRD), both conducted in situ.[3] Due to the templating effect from the fcc-Rh core, the Ru atoms in the shell were crystallized in an fcc lattice, instead of the hexagonal-close packed (hcp) phase typical of bulk Ru. The fcc-Ru phase is expected to exhibit superior catalytic activities toward an array of reactions when compared with the hcp counterpart, but the former is a kinetically controlled product.[23,24] Based on DFT calculations, the hcp phase is more stable than the fcc phase for Ru nanocrystals with a relatively large size (>6 nm) because of the greater cohesive energy in hcp lattice.[25,26] Upon heating, the Rh@Ru core−shell nanocrystals could maintain their octahedral shape up to 400 °C and then transform into spheroids at higher temperatures as a result of rounding at the corners and edges (Figure 5D). Energy-dispersive X-ray (EDX) mapping of the nanocrystals annealed at 400 °C confirmed the well-preserved core−shell structure, with the surface still dominated by Ru while the Rh core was slightly enlarged owing to atomic interdiffusion. The in situ XRD data shown in Figure 5E indicate that the fcc structure of the Ru shell was well preserved up to 400 °C, followed by phase transition from fcc to hcp at 500 °C. These

https://dx.doi.org/10.1021/acs.accounts.0c00640
Acc. Chem. Res. 2021, 54, 1−10

results confirmed that both the shape and fcc structure of the Rh@Ru octahedral nanocrystals could be maintained up to 400 °C, suggesting their potential use as catalysts toward reactions conducted at elevated temperatures, including the Fischer−Tropsch process.

4. HOLLOW NANOCRYSTALS

Hollow nanocrystals made of noble metals, including nanocages and nanoframes, have received interest for a variety of applications such as catalysis and biomedicine.[27−29] Compared with solid nanocrystals, the highly open structure associated with hollow nanocrystals can greatly boost their mass activity toward a catalytic reaction, but will also make them more vulnerable to fragmentation when thermally activated, compromising their thermal stability.

We conducted a set of in situ TEM experiments to analyze the behaviors of Pt nanocages with different shapes when subjected to direct heating.[30] As shown in Figure 6, the pores in the walls of all the nanocages were gradually enlarged upon heating, increasing the ridge thickness and transforming the structure into a nanoframe, followed by fragmentation into small solid particles. Considering the much greater surface-to-volume ratio of nanocages relative to their solid counterparts, the above transformation was able to reduce the total free energy of the system. When the atoms situated on the side faces migrated to the edges for the formation of nanoframes, the specific surface area and thus total surface free energy of the nanocage could be substantially reduced. With enough thermal energy provided, the nanoframe finally fragmented into smaller, solid particles.

Despite their similarity in thermal behavior, the temperature at which the transformation started to occur was found to be dependent on the shape of the nanocages, with the stabilities of Pt nanocages increasing in the order of icosahedron < octahedron < cube.[30] The difference in the thermal stabilities could be attributed to the location of the holes on different nanocages and the associated hole curvature, as well as the strain energy, which could contribute to the hole growth and edge atom retraction.[31] The synthesis of Pt nanocages typically involves removal of atoms from the core of the corresponding core−shell nanocrystals through chemical etching in the presence of Br^- or other halide ions. Due to the selective adsorption of Br^- ions to Pt{100}, holes were initiated on the side faces of a cube while the vertices of an octahedron during the etching process. The latter would experience accelerated atom diffusion, as driven by the hole curvature, resulting in the growth of holes on an octahedral nanocage occurring at a lower temperature than that on a cubic nanocage.[31] Owing to the inclusion of twin defects and thus additional surface strain, the stability of icosahedral nanocages was even more greatly compromised relative to their single-crystal counterparts. Although all the Pt nanocages could stay intact up to 150 °C, their stability was largely inferior to the Pd@Pt core−shell nanocrystals,[2] suggesting that more efforts should be devoted to improving the stability of hollow nanocrystals. Based on the mechanism proposed above, new opportunities will arise if we can precisely control the locations of the holes created during an etching process by optimizing the capping agent and/or etchant.

In addition to the shape and morphology deformation, phase transition could also occur to hollow nanocrystals when subjected to elevated temperatures. A notable example can be found in the Ru nanocages and nanoframes in an fcc

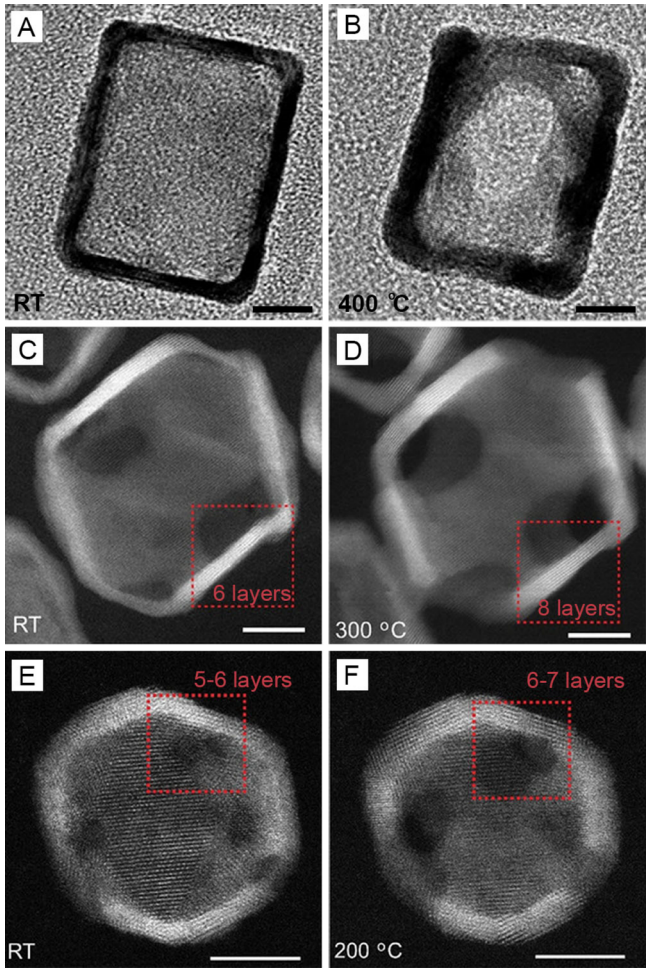

Figure 6. (A, B) High-resolution TEM images of a Pt cubic nanocage (A) before and (B) after heating at 400 °C for 60 min, respectively, showing the transformation from nanocage to nanoframe. (C−F) HAADF-STEM images of Pt nanocages with a shape of (C, D) octahedron and (E, F) icosahedron, respectively, before and after thermal annealing at the marked temperatures, showing the enlargement in pore size and increase in ridge thickness. The scale bars in all panels are 5 nm. Acceleration voltages of 300 and 200 kV were used for the high- resolution TEM and STEM imaging, respectively. Modified with permission from ref 30. Copyright 2018 Wiley-VCH.

structure.[4,32,33] By integrating XRD with in situ heating, we investigated the thermal stability of fcc-Ru cuboctahedral nanoframes[33] and nanocages in the shape of an octahedron[32] or icosahedron.[4] Despite the difference in shape and morphology, all the Ru hollow nanocrystals could preserve their shape and fcc structure up to 300 °C. Upon heating to 350 °C, as shown in Figure 7A and B, the nanocages were broken into small fragments along with the loss of shape. In addition, the hcp-(101) peak appeared in the XRD pattern (Figure 7C), indicating the occurrence of phase transition. When the temperature was elevated to 400 °C and higher, the characteristic peaks of fcc-Ru disappeared while the XRD pattern was dominated by hcp-Ru, suggesting the complete transformation of crystal structure from fcc to hcp. Although the exact mechanism is yet to be resolved, the phase stability of Ru hollow nanocrystals shows no direct correlation with their shape or morphology. The same transformation temperature for all the Ru hollow nanocrystals can probably be attributed to

https://dx.doi.org/10.1021/acs.accounts.0c00640
Acc. Chem. Res. 2021, 54, 1−10

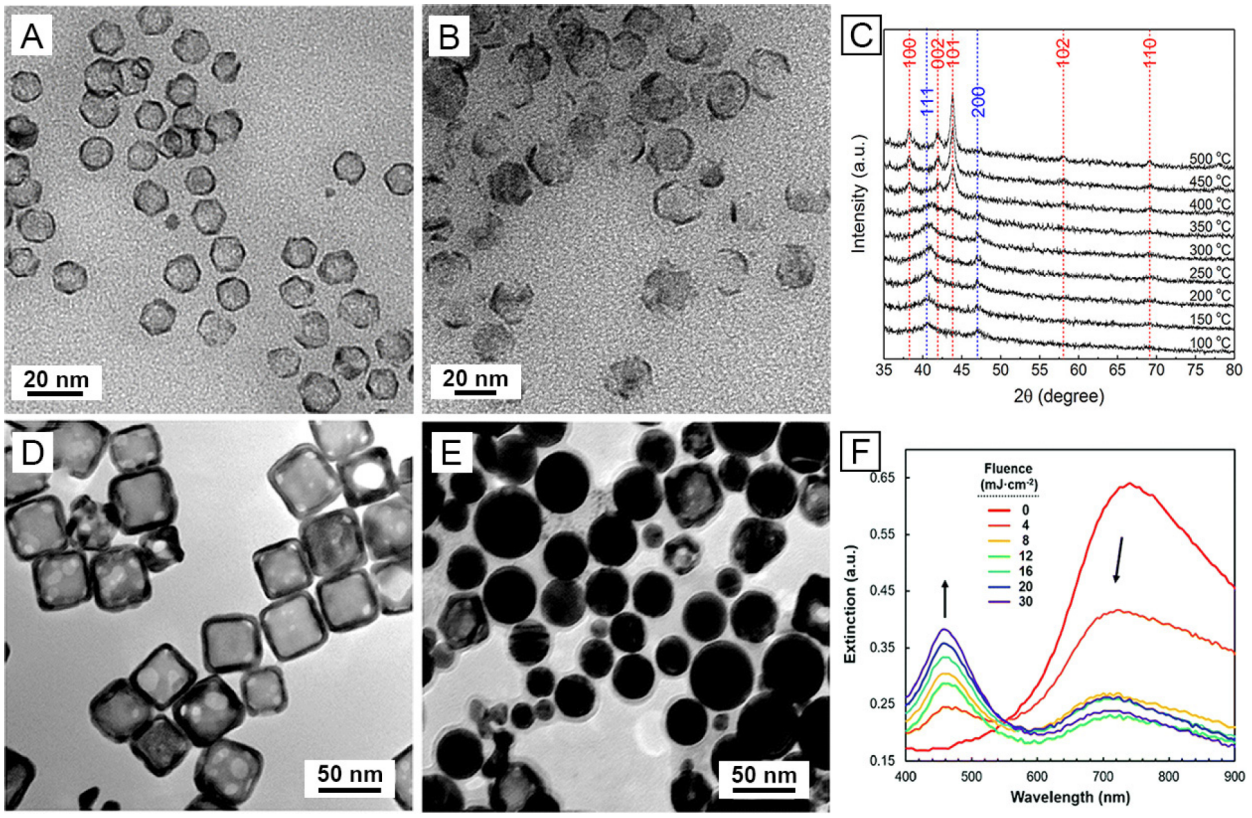

Figure 7. (A, B) TEM images of Ru icosahedral nanocages (A) before and (B) after heating at 350 °C for 1 h, respectively. The nanocrystals were heated under Ar atmosphere and then cooled down to room temperature and analyzed by TEM. (C) In situ XRD patterns of the fcc-Ru icosahedral nanocages heated to different temperatures. The characteristic peaks of fcc- and hcp-Ru are marked by blue and red dashed lines, respectively. (D, E) TEM images of Au−Ag nanocages (D) before and (E) after irradiation by 300 laser pulses at a fluence of 20 mJ cm^{-2}, respectively. (F) UV−vis spectra recorded from the Au−Ag nanocages after 300 pulses of laser irradiation at different fluences. Reproduced with permission from (A−C) ref 4 and (D−F) ref 8. Copyrights 2018 American Chemical Society and 2019 Royal Society of Chemistry, respectively.

the same energy barrier that Ru atoms have to overcome for diffusion and rearrangement. Similar to Pt nanocages, the shape and phase stability of Ru hollow nanocrystals is inferior to the solid, core−shell nanocrystals.[3] As discussed in section 3, the Rh@Ru octahedral nanocrystals could maintain their shape and fcc structure up to 400 °C, 100 °C higher than the transition point of Ru nanocages. The enhanced stability of the core−shell nanocrystals might arise from their thicker shell relative to the nanocages (4.5 vs 1.1 nm) as well as the slow interdiffusion between Rh and Ru atoms. Both factors help preserve the fcc lattice.

Besides direct heating, nanocrystals capable of converting light to heat could also undergo shape and morphology transformations under light irradiation. Nanocages made of plasmonic metals, such as Au and Ag, have received interest in biomedical applications for both diagnostics and therapeutics.[34−38] However, their structure−stability relationship needs to be fully explored in order to optimize their performance. To this end, we examined the photothermal transformation of Au−Ag nanocages when irradiated by a pulsed laser at 750 nm.[8] As shown in Figure 7D and E, after exposure to 300 laser pulses at a fluence of 20 mJ cm^{-2}, the Au−Ag cubic nanocages evolved into pseudospherical, solid nanoparticles with a polycrystalline structure. In addition, their optical property changed correspondingly as the intensity of the peak at 750 nm decreased while a new peak appeared at 460 nm (Figure 7F), in agreement with the simulation based on the discrete dipole approximation method. The transformation of the Au−Ag nanocages would be accelerated when increasing the laser fluence and the number of pulses as these parameters would increase the energy deposited into the system. The photothermal transformation likely involved lattice heating because of the absorption of photons and thus electron−phonon relaxation.[39] With enough energy supplied, the atoms were allowed to diffuse across the surface of the nanocages, giving rise to the solid, pseudospherical nanoparticles favored by thermodynamics due to the reduction in total surface free energy. Another plausible explanation is that the morphological transformation was driven by the desire to minimize the electrostatic repulsion between charges in the ionized nanoparticles resulting from the laser irradiation. The photothermal transformation of Au−Ag nanocages under laser irradiation could have detrimental impact on biomedical applications relying on their plasmonic properties, such as photoacoustic imaging and cancer treatment. On the other hand, due to the inclusion of structural defects during the morphological transformation, this process may offer nanoparticles with enhanced catalytic activity.

5. CONCLUSION AND PERSPECTIVES

Most of the noble-metal nanocrystals reported in the literature are intrinsically susceptible to physical transformations because they are kinetically controlled products. The transformation is mainly driven by the goal to reduce the total free energy of the system through the reduction in surface area, elimination of facets or sites high in energy, and increase of disorder in

https://dx.doi.org/10.1021/acs.accounts.0c00640
Acc. Chem. Res. 2021, 54, 1−10

Table 1. Summary of the Thermally Driven Transformations of Nanocrystals in Terms of Shape, Structure, Elemental Distribution, and Crystal Phase, as Discussed in This Account

sample	transformation process	before transformation	after transformation	ref
Pd nanocube	heating (500 °C)	sharp corners, defected surface	truncated corners, smooth surface	15
Pd concave icosahedron	heating (up to 600 °C)	concave icosahedral shape, multiply-twinned structure	icosahedron with a rounded profile and multiply-twinned structure at 400 °C, converted to a single crystal featuring a pseudospherical shape at 600 °C	1
Pd@Pt_{4L} nanocube	heating (up to 800 °C)	core−shell structure, cubic shape	shape deformation starting from 500 °C, interdiffusion and alloying from 800 °C	2
Pd@Pt_{4L} octahedron	heating (up to 900 °C)	core−shell structure, octahedral shape	shape deformation starting from 900 °C, interdiffusion and alloying from 600 °C	2
Rh@Ru octahedron	heating (up to 800 °C)	core−shell structure, octahedral shape, fcc-Ru phase	shape deformation and crystal structure transformation from fcc to hcp at temperatures above 400 °C	3
Pt cubic nanocage	heating (up to 500 °C)	cubic cage with small pores on side faces	transforming to nanoframes with thicker edges at 400 °C, breaking into smaller particles at 500 °C	30
Pt octahedral nanocage	heating (up to 500 °C)	octahedral cage with pores at vertices	pore enlargement and edge thickening at 300 °C, collapse into smaller pieces at 400 °C	30
Pt icosahedral nanocage	heating (up to 500 °C)	icosahedral cage with multiple twin boundaries and small pores on surface	pore enlargement and edge thickening at 200 °C, collapse into smaller pieces at higher temperatures	30
Ru octahedral nanocage	heating (up to 450 °C)	octahedral cage with a porous shell, fcc-Ru phase	phase transformation from fcc to hcp at 350 °C	32
Ru icosahedral nanocage	heating (up to 500 °C)	icosahedral cage with a porous shell, fcc-Ru phase	fragmentation and crystal structure transformation from fcc to hcp at 350 °C	4
Ru cuboctahedral nanoframe	heating (up to 500 °C)	frame with a cuboctahedral shape, fcc-Ru phase	fragmentation and crystal structure transformation from fcc to hcp at 350 °C	33
Au−Ag nanocage	irradiation (300 laser pulses at a fluence up to 30 mJ cm^{-2})	cubic cage with small pores at corners and side faces	pseudospherical, solid nanoparticles with a polycrystalline structure	8

elemental distribution. When subjected to high temperatures, such a transformation will be accelerated. In general, the nanocrystals are transformed into particles with a solid, pseudospherical shape, single-crystal structure, and alloy composition. For hollow nanocrystals such as cages and frames, they can be fragmented upon thermal activation due to their large surface area to generate multiple pseudospherical particles. As for nanocrystal in a metastable crystal phase, they are supposed to evolve into the conventional bulk structure more favored by thermodynamics. Table 1 shows a summary of the transformations of nanocrystals presented in this Account. Our investigation on the physical transformations of various types of nanocrystals has demonstrated that their thermal stability is highly dependent on the size, shape, morphology, and internal structure. Such dependences need to be further explored in order to achieve a deeper understanding of their thermal behaviors. It is worth pointing out that, during TEM/STEM imaging, the electron beam may also induce shape and structural transformations in nanocrystals when it is used at a high dose rate. In our in situ heating experiments, we typically kept the beam off when heating the nanocrystals and captured the image as quickly as possible to avoid any long-time exposure of nanocrystals to the electron beam. As such, we believe that direct heating is the dominant factor contributing to the observed transformations. In addition, for all the studies discussed in this Account article, we also took high-resolution TEM images of the nanocrystals at room temperature using the same parameters as those from in situ heating experiments. No shape transformation was observed under the same electron dose rate, indicating negligible influence from the electron beam.

There is an urgent need to greatly improve the thermal stability of noble-metal nanocrystals because this parameter has a major impact on their performance in essentially all applications. Our current understanding of the parameters that affect the thermal stability of nanocrystals, as discussed above, offers some insightful guidance. In the case of core−shell nanocrystals, for example, their stability in terms of shape and composition can be augmented through shape-controlled synthesis, with octahedral and cubic shapes preferred for the preservation of shape and core−shell structure, respectively. Moreover, it was reported that melting and reconstruction tended to occur at a lower temperature on the surface of a nanocrystal than in the bulk.[40,41] As such, patching the most vulnerable sites with a more resistant material offers an effective strategy to improve the thermal stability of metal nanocrystals. In one study, we demonstrated that the thermal stability of Pd−Rh core−frame nanocubes was significantly enhanced relative to Pd nanocubes of a similar size (Figure 8).[42] When heating to 500 °C, the Pd nanocubes underwent shape deformation after only 3 min while the cubic shape of the Pd−Rh core−frame nanocubes could be maintained even after 60 min. By coating the corners and edges with Rh, the surface premelting of Pd nanocubes was substantially suppressed due to the higher melting point of Rh (1964 °C vs 1555 °C for Pd) and thus higher energy barrier to surface diffusion, leading to improved thermal stability. As such, the Pd{100} facets on the Pd@Rh nanocrystals can be used up to a higher temperature than those on Pd nanocubes. Other reports also demonstrated that the thermal stability of Ni[43] and Pt nanoparticles[44] could be significantly enhanced without compromising their catalytic activities by encapsulating them in porous oxide shells.

As our mechanistic understanding of the shape and structural transformations is deepened, noble-metal nanocrystals with improved thermal stability could be eventually achieved through rational design. The enhanced stability would play a major role in maintaining their performance in applications involving harsh environments, such as thermal catalysis and photothermal therapy. It is hoped that this

https://dx.doi.org/10.1021/acs.accounts.0c00640
Acc. Chem. Res. 2021, 54, 1−10

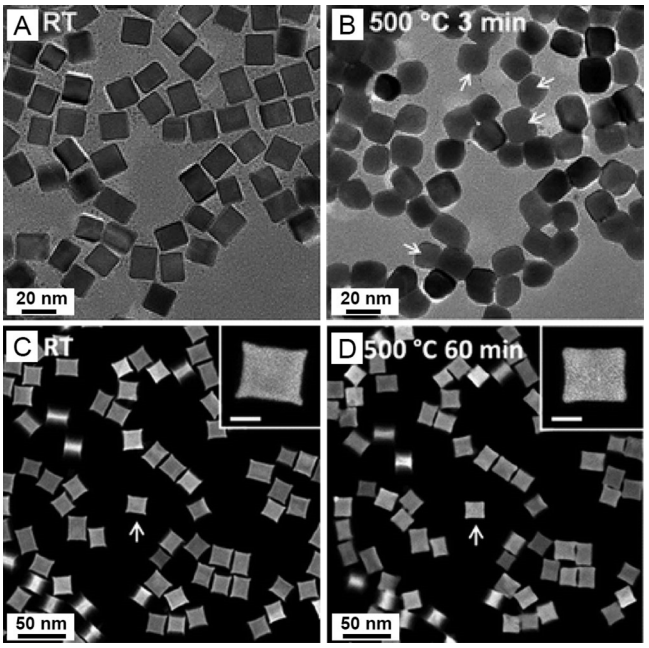

Figure 8. (A, B) TEM images of Pd nanocubes (A) before and (B) after heating at 500 °C for 3 min, respectively, suggesting the shape deformation at an elevated temperature. (C, D) HAADF-STEM images of Pd−Rh core−frame nanocubes (C) before and (D) after heating at 500 °C for 60 min, respectively, demonstrating the enhanced shape stability. The scale bars in the insets are 10 nm. An acceleration voltage of 200 kV was used for TEM and STEM imaging. Reproduced with permission from ref 42. Copyright 2013 Royal Society of Chemistry.

Account will inspire the readers to push noble-metal nanocrystals one step closer toward practical use in various applications.

AUTHOR INFORMATION

Corresponding Author

Younan Xia − *School of Chemistry and Biochemistry and School of Chemical and Biomolecular Engineering, Georgia Institute of Technology, Atlanta, Georgia 30332, United States; The Wallace H. Coulter Department of Biomedical Engineering, Georgia Institute of Technology and Emory University, Atlanta, Georgia 30332, United States;* orcid.org/0000-0003-2431-7048; Email: younan.xia@bme.gatech.edu

Authors

Zhiheng Lyu − *School of Chemistry and Biochemistry, Georgia Institute of Technology, Atlanta, Georgia 30332, United States;* orcid.org/0000-0002-1343-4057

Ruhui Chen − *School of Chemistry and Biochemistry, Georgia Institute of Technology, Atlanta, Georgia 30332, United States*

Manos Mavrikakis − *Department of Chemical and Biological Engineering, University of Wisconsin−Madison, Madison, Wisconsin 53706, United States*

Complete contact information is available at: https://pubs.acs.org/10.1021/acs.accounts.0c00640

Author Contributions

⊥Z.L. and R.C. contributed equally to the preparation of this Account.

Notes

The authors declare no competing financial interest.

Biographies

Zhiheng Lyu received her B.S. in Chemistry from the University of Science and Technology of China in 2016. She just completed her Ph.D. study under the supervision of Prof. Xia in the School of Chemistry and Biochemistry at the Georgia Institute of Technology. Her research interest includes shape-controlled synthesis of metal nanocrystals and their utilization for energy-related applications.

Ruhui Chen received her B.E. in Macromolecular Materials and Engineering from the University of Science and Technology of China in 2017. She is pursuing her Ph.D. in Chemistry and Biochemistry at the Georgia Institute of Technology under the supervision of Prof. Xia. Her research focuses on the development of new methods for controlling the nucleation and growth of nanostructured materials.

Manos Mavrikakis received his Ph.D. in Chemical Engineering & Scientific Computing from the University of Michigan, Ann Arbor. Following postdoctoral work at the University of Delaware and the Technical University of Denmark, he joined the faculty at the University of Wisconsin—Madison in 1999. He is currently the Paul A. Elfers Professor of Chemical Engineering, and has served as the editor-in-chief of *Surface Science* since 2012.

Younan Xia received his Ph.D. in Physical Chemistry from Harvard University in 1996 (with Whitesides). He started as an Assistant Professor of Chemistry at the University of Washington, Seattle in 1997 and then joined the Department of Biomedical Engineering at Washington University in St. Louis in 2007 as the James M. McKelvey Professor. Since 2012, he has held the position of Brock Family Chair and GRA Eminent Scholar in Nanomedicine at the Georgia Institute of Technology. He served as an Associate Editor of Nano Letters from 2002−2019.

ACKNOWLEDGMENTS

This work was supported in part by the NSF (CHE-1804970, CHE-1505441, DMR-1505400, and DMR-1215034) and startup funds from the Georgia Institute of Technology. We thank our collaborators for their invaluable contributions to these studies.

REFERENCES

(1) Gilroy, K. D.; Elnabawy, A. O.; Yang, T. H.; Roling, L. T.; Howe, J.; Mavrikakis, M.; Xia, Y. Thermal Stability of Metal Nanocrystals: An Investigation of the Surface and Bulk Reconstructions of Pd Concave Icosahedra. *Nano Lett.* **2017**, *17*, 3655−3661.

(2) Vara, M.; Roling, L. T.; Wang, X.; Elnabawy, A. O.; Hood, Z. D.; Chi, M.; Mavrikakis, M.; Xia, Y. Understanding the Thermal Stability of Palladium-Platinum Core-Shell Nanocrystals by *In Situ* Transmission Electron Microscopy and Density Functional Theory. *ACS Nano* **2017**, *11*, 4571−4581.

(3) Zhao, M.; Chen, Z.; Lyu, Z.; Hood, Z. D.; Xie, M.; Vara, M.; Chi, M.; Xia, Y. Ru Octahedral Nanocrystals with a Face-Centered Cubic Structure, {111} Facets, Thermal Stability up to 400 °C, and Enhanced Catalytic Activity. *J. Am. Chem. Soc.* **2019**, *141*, 7028−7036.

(4) Zhao, M.; Xu, L.; Vara, M.; Elnabawy, A. O.; Gilroy, K. D.; Hood, Z. D.; Zhou, S.; Figueroa-Cosme, L.; Chi, M.; Mavrikakis, M.; Xia, Y. Synthesis of Ru Icosahedral Nanocages with a Face-Centered-Cubic Structure and Evaluation of Their Catalytic Properties. *ACS Catal.* **2018**, *8*, 6948−6960.

(5) Xia, Y.; Xia, X.; Peng, H. C. Shape-Controlled Synthesis of Colloidal Metal Nanocrystals: Thermodynamic versus Kinetic Products. *J. Am. Chem. Soc.* **2015**, *137*, 7947−7966.
(6) Martinez-Canales, M.; Pickard, C. J.; Needs, R. J. Thermodynamically Stable Phases of Carbon at Multiterapascal Pressures. *Phys. Rev. Lett.* **2012**, *108*, 045704.
(7) Scarselli, M.; Castrucci, P.; De Crescenzi, M. Electronic and Optoelectronic Nano-Devices Based on Carbon Nanotubes. *J. Phys.: Condens. Matter* **2012**, *24*, 313202.
(8) Hood, Z. D.; Kubelick, K. P.; Gilroy, K. D.; Vanderlaan, D.; Yang, X.; Yang, M.; Chi, M.; Emelianov, S. Y.; Xia, Y. Photothermal Transformation of Au-Ag Nanocages under Pulsed Laser Irradiation. *Nanoscale* **2019**, *11*, 3013−3020.
(9) Moon, G. D.; Choi, S. W.; Cai, X.; Li, W.; Cho, E. C.; Jeong, U.; Wang, L. V.; Xia, Y. A New Theranostic System Based on Gold Nanocages and Phase-Change Materials with Unique Features for Photoacoustic Imaging and Controlled Release. *J. Am. Chem. Soc.* **2011**, *133*, 4762−4765.
(10) Yang, X.; Gilroy, K. D.; Vara, M.; Zhao, M.; Zhou, S.; Xia, Y. Gold Icosahedral Nanocages: Facile Synthesis, Optical Properties, and Fragmentation under Ultrasonication. *Chem. Phys. Lett.* **2017**, *683*, 613−618.
(11) Schulz, H. Short History and Present Trends of Fischer−Tropsch Synthesis. *Appl. Catal., A* **1999**, *186*, 3−12.
(12) Freund, H. J.; Meijer, G.; Scheffler, M.; Schlögl, R.; Wolf, M. CO Oxidation as a Prototypical Reaction for Heterogeneous Processes. *Angew. Chem., Int. Ed.* **2011**, *50*, 10064−10094.
(13) Ratnasamy, C.; Wagner, J. Water Gas Shift Catalysis. *Catal. Rev.: Sci. Eng.* **2009**, *51*, 325−440.
(14) Kitano, M.; Kanbara, S.; Inoue, Y.; Kuganathan, N.; Sushko, P. V.; Yokoyama, T.; Hara, M.; Hosono, H. Electride Support Boosts Nitrogen Dissociation over Ruthenium Catalyst and Shifts the Bottleneck in Ammonia Synthesis. *Nat. Commun.* **2015**, *6*, 6731.
(15) Lim, B.; Kobayashi, H.; Camargo, P. H. C.; Allard, L. F.; Liu, J.; Xia, Y. New Insights into the Growth Mechanism and Surface Structure of Palladium Nanocrystals. *Nano Res.* **2010**, *3*, 180−188.
(16) Zhang, H.; Jin, M.; Xia, Y. Noble-Metal Nanocrystals with Concave Surfaces: Synthesis and Applications. *Angew. Chem., Int. Ed.* **2012**, *51*, 7656−7673.
(17) Baletto, F.; Ferrando, R.; Fortunelli, A.; Montalenti, F.; Mottet, C. Crossover among Structural Motifs in Transition and Noble-Metal Clusters. *J. Chem. Phys.* **2002**, *116*, 3856−3863.
(18) Baletto, F.; Ferrando, R. Structural Properties of Nanoclusters: Energetic, Thermodynamic, and Kinetic Effects. *Rev. Mod. Phys.* **2005**, *77*, 371−423.
(19) Wang, R.; Zhang, H.; Farle, M.; Kisielowski, C. Structural Stability of Icosahedral FePt Nanoparticles. *Nanoscale* **2009**, *1*, 276−279.
(20) Fan, Z.; Zhang, H. Template Synthesis of Noble Metal Nanocrystals with Unusual Crystal Structures and Their Catalytic Applications. *Acc. Chem. Res.* **2016**, *49*, 2841−2850.
(21) Xia, Y.; Gilroy, K. D.; Peng, H. C.; Xia, X. Seed-Mediated Growth of Colloidal Metal Nanocrystals. *Angew. Chem., Int. Ed.* **2017**, *56*, 60−95.
(22) Gilroy, K. D.; Ruditskiy, A.; Peng, H. C.; Qin, D.; Xia, Y. Bimetallic Nanocrystals: Syntheses, Properties, and Applications. *Chem. Rev.* **2016**, *116*, 10414−10472.
(23) Zhao, M.; Xia, Y. Crystal-Phase and Surface-Structure Engineering of Ruthenium Nanocrystals. *Nat. Rev. Mater.* **2020**, *5*, 440−459.
(24) Li, W. Z.; Liu, J. X.; Gu, J.; Zhou, W.; Yao, S. Y.; Si, R.; Guo, Y.; Su, H. Y.; Yan, C. H.; Li, W. X.; Zhang, Y. W.; Ma, D. Chemical Insights into the Design and Development of Face-Centered Cubic Ruthenium Catalysts for Fischer−Tropsch Synthesis. *J. Am. Chem. Soc.* **2017**, *139*, 2267−2276.
(25) Nanba, Y.; Ishimoto, T.; Koyama, M. Structural Stability of Ruthenium Nanoparticles: A Density Functional Theory Study. *J. Phys. Chem. C* **2017**, *121*, 27445−27452.
(26) Sun, C. Q. Thermal Stability: Atomic Cohesive Energy. In *Relaxation of the Chemical Bond*; Springer Singapore: Singapore, 2014; Chapter 14.
(27) Zhao, M.; Wang, X.; Yang, X.; Gilroy, K. D.; Qin, D.; Xia, Y. Hollow Metal Nanocrystals with Ultrathin, Porous Walls and Well-Controlled Surface Structures. *Adv. Mater.* **2018**, *30*, 1801956.
(28) Xia, Y.; Li, W.; Cobley, C. M.; Chen, J.; Xia, X.; Zhang, Q.; Yang, M.; Cho, E. C.; Brown, P. K. Gold Nanocages: From Synthesis to Theranostic Applications. *Acc. Chem. Res.* **2011**, *44*, 914−924.
(29) Mahmoud, M. A.; El-Sayed, M. A. Gold Nanoframes: Very High Surface Plasmon Fields and Excellent Near-Infrared Sensors. *J. Am. Chem. Soc.* **2010**, *132*, 12704−12710.
(30) Vara, M.; Wang, X.; Howe, J.; Chi, M.; Xia, Y. Understanding the Stability of Pt-Based Nanocages under Thermal Stress Using In Situ Electron Microscopy. *ChemNanoMat* **2018**, *4*, 112−117.
(31) Thompson, C. V. Solid-State Dewetting of Thin Films. *Annu. Rev. Mater. Res.* **2012**, *42*, 399−434.
(32) Zhao, M.; Elnabawy, A. O.; Vara, M.; Xu, L.; Hood, Z. D.; Yang, X.; Gilroy, K. D.; Figueroa-Cosme, L.; Chi, M.; Mavrikakis, M.; Xia, Y. Facile Synthesis of Ru-Based Octahedral Nanocages with Ultrathin Walls in a Face-Centered Cubic Structure. *Chem. Mater.* **2017**, *29*, 9227−9237.
(33) Zhao, M.; Hood, Z. D.; Vara, M.; Gilroy, K. D.; Chi, M.; Xia, Y. Ruthenium Nanoframes in the Face-Centered Cubic Phase: Facile Synthesis and Their Enhanced Catalytic Performance. *ACS Nano* **2019**, *13*, 7241−7251.
(34) Chen, J.; Wang, D.; Xi, J.; Au, L.; Siekkinen, A.; Warsen, A.; Li, Z. Y.; Zhang, H.; Xia, Y.; Li, X. Immuno Gold Nanocages with Tailored Optical Properties for Targeted Photothermal Destruction of Cancer Cells. *Nano Lett.* **2007**, *7*, 1318−1322.
(35) Cobley, C. M.; Au, L.; Chen, J.; Xia, Y. Targeting Gold Nanocages to Cancer Cells for Photothermal Destruction and Drug Delivery. *Expert Opin. Drug Delivery* **2010**, *7*, 577−587.
(36) Cheng, H.; Huo, D.; Zhu, C.; Shen, S.; Wang, W.; Li, H.; Zhu, Z.; Xia, Y. Combination Cancer Treatment through Photothermally Controlled Release of Selenous Acid from Gold Nanocages. *Biomaterials* **2018**, *178*, 517−526.
(37) Wang, Y.; Black, K. C. L.; Luehmann, H.; Li, W.; Zhang, Y.; Cai, X.; Wan, D.; Liu, S. Y.; Li, M.; Kim, P.; Li, Z. Y.; Wang, L. V.; Liu, Y.; Xia, Y. Comparison Study of Gold Nanohexapods, Nanorods, and Nanocages for Photothermal Cancer Treatment. *ACS Nano* **2013**, *7*, 2068−2077.
(38) Li, W.; Brown, P. K.; Wang, L. V.; Xia, Y. Gold Nanocages as Contrast Agents for Photoacoustic Imaging. *Contrast Media Mol. Imaging* **2011**, *6*, 370−377.
(39) Link, S.; Burda, C.; Mohamed, M. B.; Nikoobakht, B.; El-Sayed, M. A. Laser Photothermal Melting and Fragmentation of Gold Nanorods: Energy and Laser Pulse-Width Dependence. *J. Phys. Chem. A* **1999**, *103*, 1165−1170.
(40) Mejía-Rosales, S. J.; Fernández-Navarro, C.; Pérez-Tijerina, E.; Montejano-Carrizales, J. M.; José-Yacamán, M. Two-Stage Melting of Au-Pd Nanoparticles. *J. Phys. Chem. B* **2006**, *110*, 12884−12889.
(41) Lewis, L. J.; Jensen, P.; Barrat, J. L. Melting, Freezing, and Coalescence of Gold Nanoclusters. *Phys. Rev. B: Condens. Matter Mater. Phys.* **1997**, *56*, 2248−2257.
(42) Lu, N.; Wang, J.; Xie, S.; Xia, Y.; Kim, M. J. Enhanced Shape Stability of Pd-Rh Core-Frame Nanocubes at Elevated Temperature: In Situ Heating Transmission Electron Microscopy. *Chem. Commun.* **2013**, *49*, 11806−11808.
(43) Zhu, S.; Lian, X.; Fan, T.; Chen, Z.; Dong, Y.; Weng, W.; Yi, X.; Fang, W. Thermally Stable Core-Shell Ni/Nanorod-CeO_2@SiO_2 Catalyst for Partial Oxidation of Methane at High Temperatures. *Nanoscale* **2018**, *10*, 14031−14038.
(44) An, K.; Zhang, Q.; Alayoglu, S.; Musselwhite, N.; Shin, J. Y.; Somorjai, G. A. High-Temperature Catalytic Reforming of n-Hexane over Supported and Core-Shell Pt Nanoparticle Catalysts: Role of Oxide-Metal Interface and Thermal Stability. *Nano Lett.* **2014**, *14*, 4907−4912.